



Ultraviolet Emission in ZnO Films Controlled by Point Defects

Chin-Ching Lin,^a Chi-Sheng Hsiao,^a San-Yuan Chen,^{a,z} and Syh-Yuh Cheng^b

^aDepartment of Materials Science and Engineering, National Chiao-Tung University, Hsinchu, Taiwan

^bMaterials Research Laboratories, Industrial Technology Research Institution, Chutung, Taiwan

The undoped ZnO films were grown on silicon (001) substrates by radio frequency magnetron sputtering. The dependence of defect formation and photoluminescence (PL) of ZnO films on the annealing temperature and oxygen mole ratio (OMR) were investigated using X-ray diffraction and PL spectra. A sharp ZnO (002) peak with a strong UV emission peak around 3.28 eV can be obtained for the films annealed in O₂ and N₂ atmospheres. However, the films annealed in nitrogen show strong deep-level emission peaks that vary with the annealing temperature. Below 850°C, Zn interstitials become the dominant point defects, but for the ZnO films annealed at higher temperatures such as 1000°C, oxygen vacancies become the predominant point defects. In contrast, in an oxygen atmosphere, a strong UV emission along with invisible deep-level peaks can be detected for ZnO films sputtered at an OMR of 5% and annealed at 850°C. This result is attributed to the enhanced crystallization and a reduced defect concentration.

© 2004 The Electrochemical Society. [DOI: 10.1149/1.1677054] All rights reserved.

Manuscript submitted April 3, 2003; revised manuscript received October 30, 2003. Available electronically March 15, 2004.

Recently, zinc oxide has attracted considerable attention because it is a potential suitable candidate for UV and blue optical applications. ZnO not only has a wide direct bandgap (3.37 eV) at room temperature but also shows a large exciton binding energy (60 meV) that is much larger than that of ZnSe (20 meV) and GaN (25 meV).¹ ZnO generally emits three luminescence bands in the UV, green, and red regions. The UV emission is considered due to exciton-related activities. However, for the visible emissions, various mechanisms have been proposed including the involvement of zinc interstitials,^{2,3} oxygen interstitials,^{4,5} zinc vacancies,^{6,7} and oxygen vacancies.^{8,9} Several important properties based on zinc oxide materials, such as electroluminescence and photoluminescence (PL), are strongly related to the defect formation. Many researchers reported that green-orange PL emitted from ZnO films is probably due to different point defects^{10,11} and strongly dependent on the predominant defect, which affects the deep-level emissions. Vanheusden *et al.*¹² and Chen *et al.*¹³ reported that oxygen vacancies are responsible for the green emission. However, Zhang *et al.*⁶ and Lin *et al.*¹⁴ considered the green emission of ZnO films to be due to zinc vacancies and antisite O_{Zn}, respectively. To obtain UV emission in ZnO films, it is important to understand the defect chemistry and to further control the defect formation through atmosphere and thermal treatment.

Sintered ZnO is a nonstoichiometric oxide at room temperature, exhibiting an n-type electrical conductivity due to an excess of zinc. The zinc excess results in intrinsic donors in ZnO, which can be assigned either to the zinc interstitials (Frenkel defect)¹⁵ or to oxygen vacancies (Schottky defect).¹⁶ These two types of point defects have similar electrical properties, making it difficult to distinguish between them. However, both point defects exhibit different defect reactions under different annealing temperatures and atmospheres. Recently, it has been revealed that the dominant point defect may vary with the annealing temperature.¹⁷ Under different annealing conditions, the crystalline characteristics of ZnO films would change to exhibit various point defects that would affect the luminescent properties.

Therefore, in this work, the relationship between the predominant defects and PL emissions in the ZnO films is focused to optimize the UV emission in ZnO films. X-ray diffraction (XRD) and room-temperature PL spectroscopy are used to study the influence of film processes and annealing conditions on the characteristics of UV and deep-level emissions in ZnO films. The role of the predominant point defects in the as-grown ZnO films on Si substrates is investigated to provide an intuition for improving the PL properties in ZnO films.

Experimental

The ZnO thin films (~100 nm) were deposited on 4 in. diam Si substrates by radio frequency (rf) magnetron sputtering using 99.99% ZnO as the target. The growth chamber was evacuated by a turbo pump and a mechanical pump. The gas mole ratio of oxygen to argon (OMR) was varied in the range of 0-72%. The silicon substrates were cleaned by the usual semiconductor technology before loading into the chamber. The sputtering conditions were optimized at a substrate temperature of 50°C, an rf power of 50 W, a sputtering pressure of 10 mTorr, and a sputtering time of 40 min. After sputtering, the as-grown films were cut into several pieces and then annealed at 500, 850, and 1000°C for 20 min under pure oxygen and nitrogen atmospheres, respectively. The film thickness was measured by a surface profilometer (Sloan Dektak 3030), and the surface morphology was examined by field-emission-scanning electron microscopy (FE-SEM, S-4100). The crystal structure was determined using a Siemens D5000 X-ray diffractometer with Cu K α radiation and a Ni filter. The PL measurement was performed by the excitation from a 325 nm He-Cd laser at room temperature.

Results and Discussion

Figure 1 shows the XRD patterns of ZnO films sputtered at an OMR of 0, 5, 20, 50, and 72%, and then annealed at 850°C in N₂ and O₂ atmospheres. Only a sharp (002) diffraction peak at 2 θ ~ 34.4° can be detected for both atmospheres. It indicates that a well-defined and oriented ZnO film has been obtained. However, with an increase of the OMR ratio, the intensity of the ZnO (002) diffraction peak is reduced. This reveals that the crystallinity of the ZnO films is hindered at a high oxygen pressure. As shown in Fig. 1, although the film crystallinity is not sensitive to the annealing atmosphere, the values (0.22, 0.18, 0.25, 0.28, and 0.5°) of full width at half-maximum (fwhm) for the ZnO (002) diffraction peak change with the OMR ratios of 0, 5, 20, 50, and 72%, respectively. The best sputtered ZnO film appears at the OMR of 5%, which is probably related to the relative ratio of Zn to ZnO as reported by Fujimura *et al.*¹⁸ Therefore, the optimum sputtering atmosphere with the OMR of 5% is used here to study the effect of annealing temperature on the film crystallinity, unless otherwise noted.

Figure 2 illustrates that the intensity of the (002) diffraction peak varies with annealing temperature. When the sputtered ZnO films are annealed below 850°C, the (002) peak intensity increases with annealing temperature up to 850°C in both N₂ and O₂ atmospheres because of the enhanced film crystallite and grain size. Above 850°C, it decreases. The smallest fwhm value in the ZnO films is obtained at 850°C. This indicates that although a higher annealing temperature can improve the crystallization of the as-grown ZnO films, as the annealing temperature exceeds 850°C, especially above

^z E-mail: sychen@cc.nctu.edu.tw

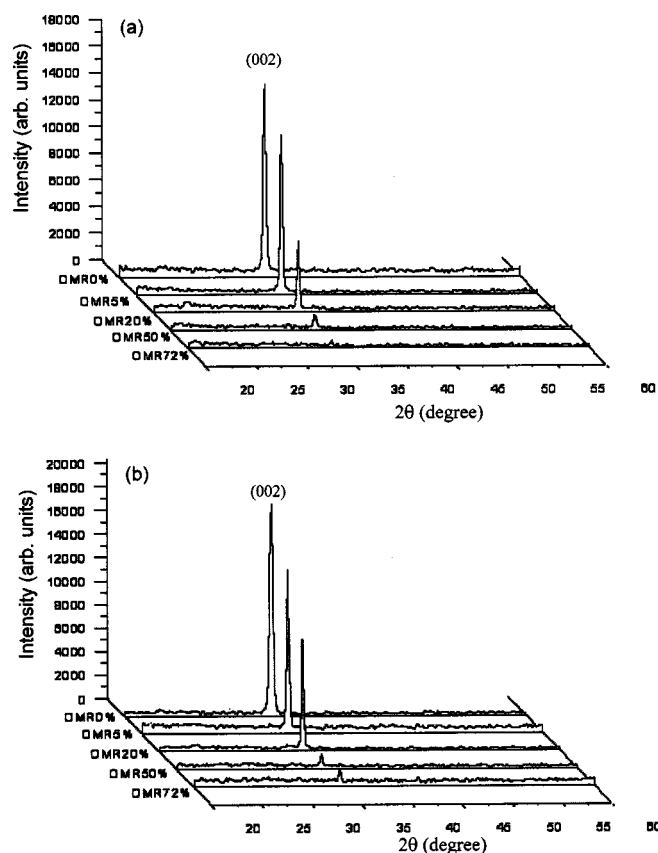


Figure 1. XRD patterns of ZnO films as function of OMR conditions after annealing at 850°C in (a) nitrogen and (b) oxygen atmospheres.

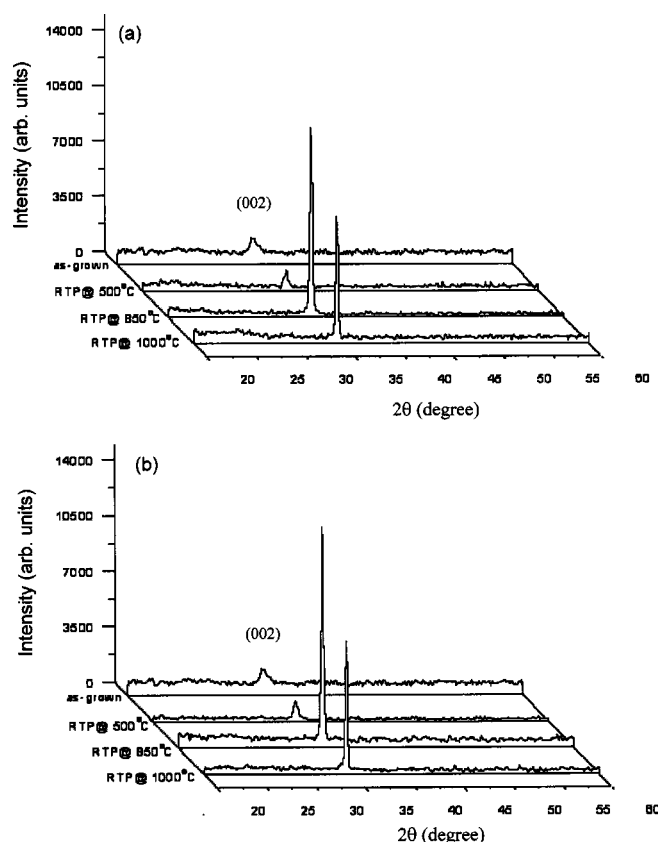


Figure 2. XRD patterns of ZnO films sputtered at OMR 5% and annealed at different temperatures in (a) nitrogen and (b) oxygen atmospheres.

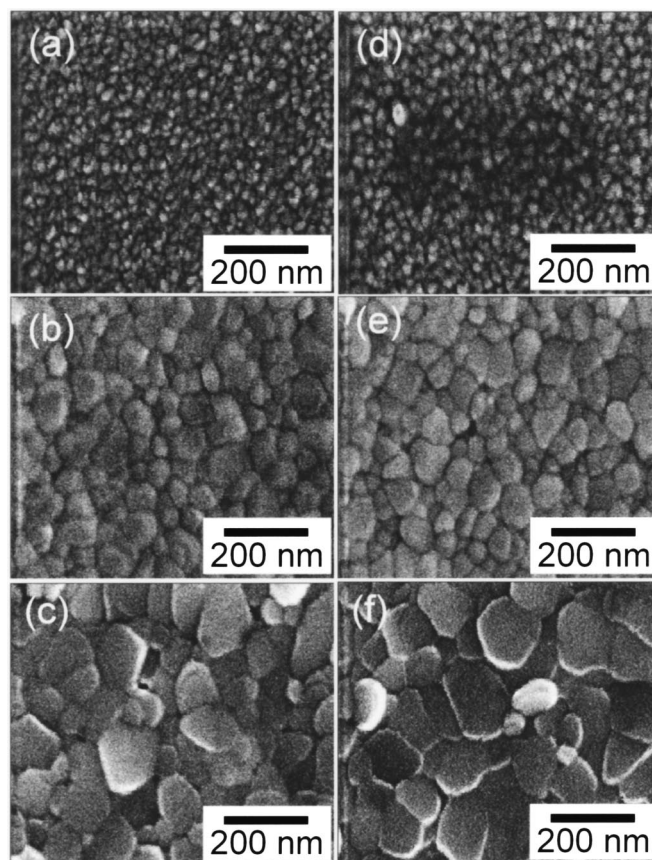


Figure 3. FE-SEM surface morphology of OMR 5%-treated ZnO films annealed under various conditions: (a) 500°C in N₂, (b) 850°C in N₂, (c) 1000°C in N₂, (d) 500°C in O₂, (e) 850°C in O₂, and (f) 1000°C in O₂.

1000°C, the crystallinity of the ZnO films may deteriorate by either crystalline lattice defects¹⁹ or thermal microstrain due to structure distortion. Therefore, the surface structure and grain morphology in ZnO films are further modified, as illustrated in Fig. 3, where a pill-like structure is shown. The formation of the pill-like structure may be related to the surface free energy and crystalline lattice defects, because numerous zinc elements are vaporized from the ZnO films at such a high annealing temperature. Therefore, under these conditions, more point defects are produced in the ZnO films.

For wide-gap semiconductors, PL emission is one of the most important properties of ZnO. Figure 4 shows the room-temperature PL spectra of the as-grown ZnO films sputtered under various OMR conditions. The peak intensity of the deep-level emission around ~600 nm changes with the OMR, and the weakest one appears at an OMR of 20%. We can consider that some of the point defects, such as oxygen vacancies and zinc interstitials, compensate each other at a certain oxygen pressure. Furthermore, as one can see, along with the decrease in deep-level emission peaks, the peak intensity of the UV emission at ~382 nm increases.

Figure 5 shows the room-temperature PL spectra of the ZnO films sputtered under various OMR values and then annealed at 850°C in N₂ and O₂ atmospheres. A strong PL emission peak corresponding to UV emission, in contrast to that of the as-grown films, appears around 378–382 nm; this peak should be a near-band-edge emission of ZnO films due to an exciton-related activity.²⁰ As shown in Fig. 5a for the films annealed in N₂ atmosphere, a very strong UV peak and a relatively low deep-level emission (528 nm) occur at an OMR of 5%. However, under these conditions (annealed in N₂ atmosphere), for the ZnO film sputtered at an OMR of 20%, the UV emission peak becomes weak and a broader deep-level emission appears around 533 nm, compared to those sputtered at other OMR

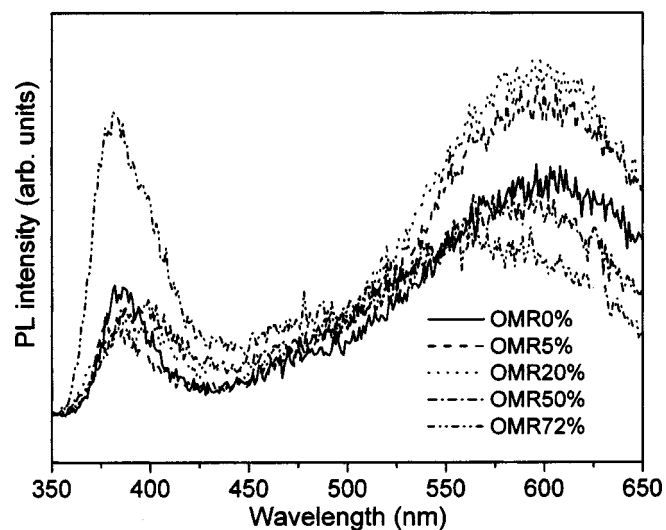


Figure 4. Room-temperature PL spectra of the as-grown ZnO films under various OMR conditions.

ratios. However, for the sputtered ZnO films annealed in O_2 atmosphere, Fig. 5b shows that the UV peak not only becomes sharper at the OMR of 5%, but also that the deep-level emission at ~ 533 nm is barely detected at the OMR of 20%. This phenomenon reveals that the deep-level emission can be reduced by controlling the OMR ratio and annealing conditions.

ZnO films can display three major PL peaks, a UV (near-band-edge) emission peak, a green emission peak, and a red emission peak. The green and red emissions are generally associated with zinc interstitials and oxygen vacancies in the ZnO lattice. Several authors have reported that the green luminescence corresponds to a transition from Zn^+ to Zn^{2+} ,¹⁷ but Riehl *et al.* attributed the green luminescence center to the oxygen vacancies (V_o^{2+}).²¹ However, we found that the dominant defect varies with the annealing conditions. As annealed in nitrogen atmosphere, a deep-level emission peak around 2.06 eV was observed for both as-grown and 500°C annealed ZnO films, as illustrated in the inset of Fig. 6. With increasing annealing temperature, at 850°C, the deep-level emission peak shifts to 2.35 eV and then again decreases to 2.26 eV at 1000°C, indicating that the dominant point defects can be controlled by changing the annealing temperature. The temperature dependence of the predominant defect in ZnO films can be further elucidated as follows.

The deep-level emission is known to be influenced by the formation of point defects. For ZnO, several reports suggested that the deep-level emission results from point defects such as the V_o^{2+} , Zn_i^{2+} , and V_{Zn}^{2+} . For the as-grown ZnO films deposited by rf magnetron sputtering, the chemical component of ZnO films is usually nonstoichiometric with oxygen insufficient and Zn interstitials predominating. However, in our case, the oxygen vacancies are considered to be the predominant point defects in the as-grown ZnO films, because the films were sputtered at an OMR of 5% (the chamber ambient is close to pure argon), and the energy level of 2.05 eV corresponds to the transition of oxygen vacancies.¹⁷ For the samples annealed below 500°C, a very weak emission was observed that was the same as for the as-grown films, because the structure characterization of ZnO film annealed below 500°C is very similar to that of the as-grown one. Therefore, in this condition, the predominant point defects are still oxygen vacancies. However, with an increase in annealing temperature, some lattice and surface defects can be removed, and the ZnO film may be rearranged into a more perfect structure, indicating that the role of predominant point defects may be different.

As the as-grown ZnO film was annealed at a high temperature in N_2 atmosphere, the nitrogen gas may be ionized as reported by

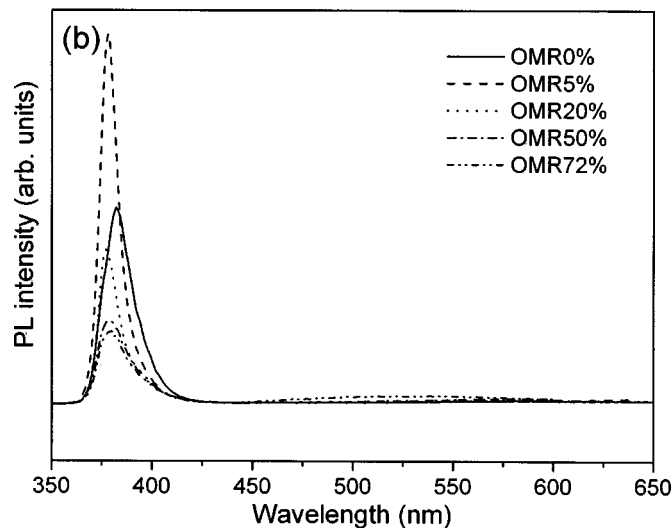
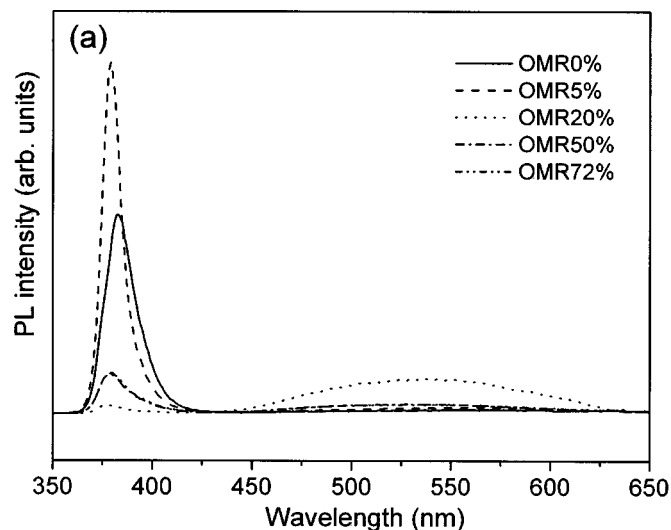


Figure 5. Room-temperature PL spectra of ZnO films treated under different OMR conditions and annealed at 850°C in (a) N_2 and (b) O_2 atmospheres.

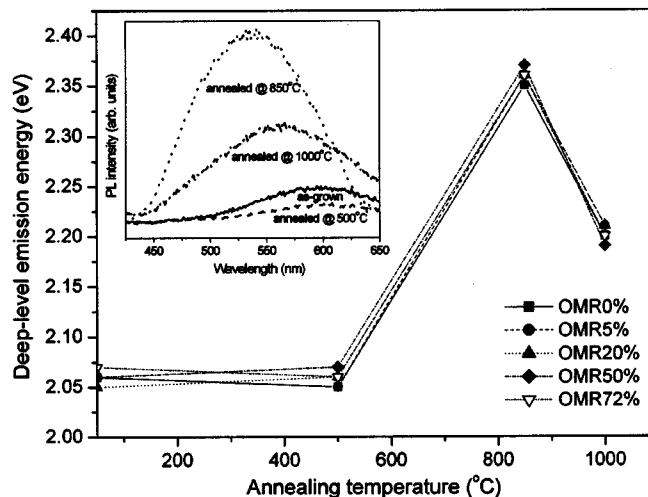


Figure 6. Defect transition of annealed ZnO films at various temperatures in N_2 atmosphere.

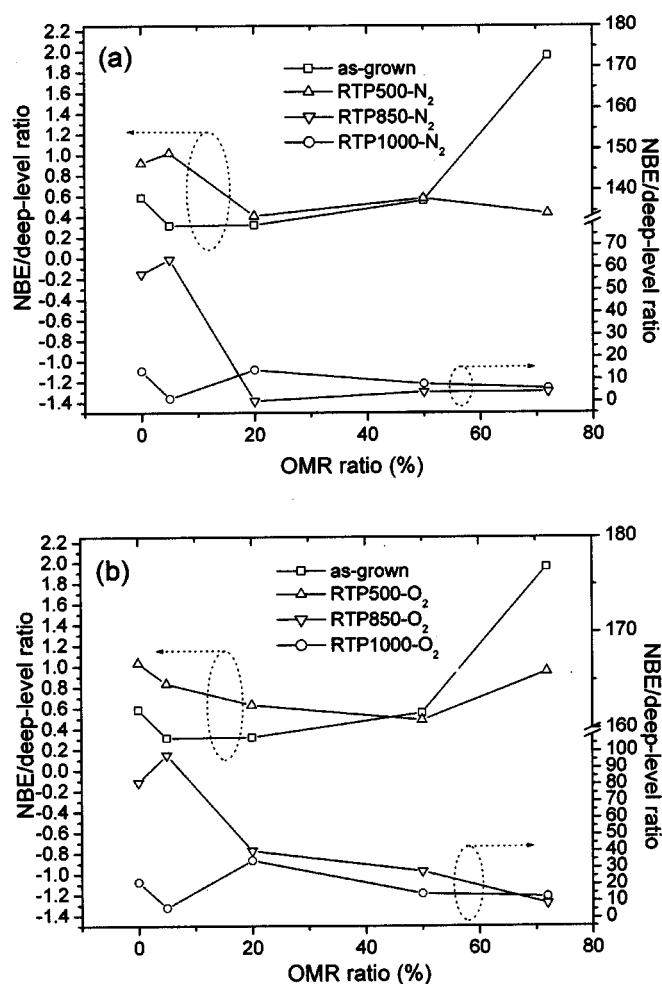


Figure 7. Relative PL intensity ratio of the UV emission to the deep-level emission for the ZnO films treated under various OMR conditions and annealed at different temperatures in (a) N_2 and (b) O_2 atmospheres.

Garces *et al.*, and the nitrogen acceptor can be effectively formed in ZnO film by thermal annealing in N_2 atmosphere in a temperature range of 600–900°C.²² If the nitrogen gas could be ionized and filled into the ZnO structure, the number of oxygen vacancies would be reduced. Furthermore, according to defect chemistry, the zinc interstitials come from the Frenkel reaction in the Zn sublattice, whereas the oxygen vacancy comes from the Schottky reaction, and it is difficult to distinguish them experimentally. However, it was reported that the Frenkel defects predominate at lower temperatures during annealing treatment of ZnO, and the Schottky defects become increasingly important at higher temperatures.²³ In other words, for the as-grown ZnO film prepared with an OMR of 5% and annealed at 850°C in N_2 atmosphere, the zinc interstitials tend to form and become the predominant point defects. As evidenced from Fig. 6, the deep-level emission at ~ 528 nm corresponds to 2.35 eV, which is primarily characteristic of the dominance of zinc interstitials. However, when the films are annealed at a higher annealing temperature such as 1000°C, a broader emission band appears around 560 nm, and the deep-level emission peak shifts from 2.35 to 2.26 eV in comparison with that at 850°C. The role of dominant point defects becomes more complicated, because a higher annealing temperature would induce a structure change and produce different types of point defects. According to the energy level, the dominant defect in the ZnO films is probably either oxygen vacancies or zinc interstitials, depending on the competition with each other. To exactly determine the possible route of defects transition, the defect concentration in ZnO films can be calculated by compar-

ing the relative PL intensity ratio of the UV emission to the deep-level emission. The PL intensity ratio changes with both OMR ratio and annealing temperatures. As illustrated in Fig. 7a for the ZnO films annealed in N_2 atmosphere, a maximum relative PL intensity ratio appears at 850°C for the films sputtered at an OMR of 5%. The value of the relative PL ratio is more than 60, much larger than that obtained by metallorganic chemical vapor deposition and molecular beam epitaxy (~ 10).²⁴ However, the relative PL value under the other conditions is below 15, except for the sample sputtered at an OMR of 0% and annealed at 850°C. In contrast, the relative PL intensity ratio can be markedly enhanced by annealing in O_2 atmosphere, as shown in Fig. 7b, because the formed oxygen vacancies in the ZnO films sputtered at a lower OMR can be further compensated in the oxygen annealing. Furthermore, the oxygen ions can combine with the zinc interstitials to form ZnO; thus, the deep-level emission can be depressed. Therefore, the defect concentration can be reduced and a sharp UV emission along with invisible deep-level peaks can be obtained for the films sputtered at an OMR of 5% and annealed at 850°C in O_2 atmosphere. The relative PL intensity ratio of the UV emission to the deep-level emission can be improved up to 98, indicating that a high-quality ZnO film with a lower defect concentration can be obtained in this work through the control of the annealing treatment.

Conclusions

ZnO films have been grown on Si(001) substrates by rf magnetron sputtering. All the ZnO films have a strongly preferred orientation (*c*-axis). Defects of both zinc interstitials and oxygen vacancies are intrinsic and hard to remove during film growth. However, we have demonstrated that it is possible to control the UV and deep-level emissions in the sputtered ZnO films by changing annealing temperatures and using different gas atmospheres. Therefore, a sharp UV emission with invisible deep-level peaks can be attained for the ZnO film sputtered at an OMR of 5% and annealed at 850°C in O_2 atmosphere.

Acknowledgment

This work was financially supported by the National Science Council of the Republic of China, Taiwan under Contract No. NSC92-2216-E-009-014.

National Chiao-Tung University assisted in meeting the publication costs of this article.

References

1. K. Hummer, *Phys. Status Solidi B*, **56**, 249 (1973).
2. S. Cho, J. Ma, Y. Kim, Y. Sun, G. K. L. Wang, and J. B. Ketterson, *Appl. Phys. Lett.*, **75**, 2761 (1999).
3. E. G. Bylander, *J. Appl. Phys.*, **49**, 1188 (1978).
4. D. Hahn and R. Nink, *Phys. Condens. Mater.*, **3**, 311 (1965).
5. M. Liu, A. H. Kitai, and P. Mascher, *J. Lumin.*, **54**, 35 (1992).
6. Y. Zhang, G. Du, D. Liu, X. Wang, Y. Ma, J. Wang, J. Yin, X. Yang, X. Hou, and S. Yang, *J. Cryst. Growth*, **243**, 439 (2002).
7. B. J. Jin, S. Im, and S. Y. Lee, *Thin Solid Films*, **366**, 107 (2000).
8. P. H. Kasai, *Phys. Rev.*, **130**, 989 (1963).
9. F. A. Kroger and H. J. Vink, *J. Chem. Phys.*, **22**, 250 (1954).
10. S. Bethke, H. Pan, and B. W. Wessies, *Appl. Phys. Lett.*, **52**, 138 (1988).
11. H.-J. Egelhaaf and D. Oelkrug, *J. Cryst. Growth*, **161**, 190 (1996).
12. K. Vanheusden, W. L. Warren, and C. H. Seager, *J. Appl. Phys.*, **79**, 7983 (1996).
13. Y. Chen, D. M. Bagnall, H. J. Koh, K. T. Park, K. Hiraga, Z. Zhu, and To. Yao, *J. Appl. Phys.*, **84**, 3912 (1998).
14. B. Lin, Z. Fu, Y. Jia, and G. Liao, *J. Electrochem. Soc.*, **148**, G110 (2001).
15. E. A. Secco and W. J. Moore, *J. Chem. Phys.*, **26**, 942 (1957).
16. G. D. Mahan, *J. Appl. Phys.*, **54**, 3825 (1983).
17. S. A. M. Lima, F. A. Sigoli, M. Jafelicci, Jr., and M. R. Davolos, *Int. J. Inorg. Mater.*, **3**, 749 (2001).
18. N. Fujimura, T. Nishihara, S. Goto, J. Xu, and T. Ito, *J. Cryst. Growth*, **130**, 169 (1993).
19. J. Hinz and K. Ellmer, *J. Appl. Phys.*, **88**, 2443 (2000).
20. Y. Chen, D. M. Bagnall, Z. Zhu, T. Sekiuchi, K.-T. Park, K. Hiraga, T. Yao, S. Koyama, M. Y. Shen, and T. Goto, *J. Cryst. Growth*, **181**, 165 (1997).
21. N. Riehl, *J. Lumin.*, **24-25**, 335 (1981).
22. N. Y. Garces, N. C. Giles, L. E. Halliburton, G. Cantwell, D. B. Eason, D. C. Reynolds, and D. C. Look, *Appl. Phys. Lett.*, **80**, 1334 (2002).
23. X. L. Wu, G. G. Siu, C. L. Fu, and H. C. Ong, *Appl. Phys. Lett.*, **78**, 2285 (2001).
24. C. R. Gorla, N. W. Emanetoglu, S. Liang, W. E. Mayo, Y. Lu, M. Wraback, and H. Shen, *J. Appl. Phys.*, **85**, 2595 (1999).